



PERGAMON

Available online at [www.sciencedirect.com](http://www.sciencedirect.com)

SCIENCE @ DIRECT®

International Journal of Rock Mechanics & Mining Sciences 40 (2003) 633–652

International Journal of  
Rock Mechanics  
and Mining Sciences

[www.elsevier.com/locate/ijrmms](http://www.elsevier.com/locate/ijrmms)

# Stability assessment of the Three-Gorges Dam foundation, China, using physical and numerical modeling—Part II: numerical modeling

Jian Liu<sup>a,b,\*</sup>, Xia-Ting Feng<sup>a</sup>, Xiu-Li Ding<sup>b</sup>

<sup>a</sup> *Institute of Rock and Soil Mechanics, The Chinese Academy of Sciences, Xiaohongshan, Hubei, Wuhan 430071, China*

<sup>b</sup> *Yangtze River Scientific Research Institute, Hubei, Wuhan 430071, China*

Accepted 31 March 2003

## Abstract

Sliding in a dam foundation along potential sliding paths is generally caused by two kinds of external factors: one is the overloading of the designed upstream hydrostatic load due to flooding; and the other is the gradual degradation of the shear strength of joints due to seepage, deformation, damage, and geochemical reactions between water and joint surface minerals. Based on the conceptualized geomechanical model of the Three-Gorges Dam, described in the Part I paper, in this Part II paper the limit equilibrium method and finite element method are used to study the effects of gradual degradation of the shear strength of joints on the stability of the dam foundation. The numerical modeling focuses on the stability conditions of the no. 3 powerhouse-dam section which are estimated to be the most critical. The constraint influences from the adjacent no. 2 and no. 4 powerhouse-dam sections are also included. The failure mechanisms, factors of safety and critical displacements of these dam sections are derived numerically as the measures for stability evaluation. The factor of safety is defined as the ratio between the combined shear strength of joints and intact rock bridges, and the mean shear stress along potential sliding path required for limit equilibrium under the designed external loads. All the results obtained from these different numerical models, together with the results of physical model tests as presented in Part I, are compared in this paper. The comparisons show that both the numerical modeling and physical modeling results support each other and demonstrate the stability of the Three-Gorges Dam foundation as designed. Nevertheless, considering the overall engineering and social–economical importance of the Three-Gorges Dam complex, some additional treatment and reinforcement measures are recommended in this paper.

© 2003 Elsevier Ltd. All rights reserved.

**Keywords:** Three-Gorges Dam; Stability assessment; Numerical modeling; Limit equilibrium analyses; Finite element method; Gently dipping joints; Rock bridges

## 1. Introduction

To assess the stability of the Three-Gorges Dam foundation, comprehensive physical modeling was conducted. The geological features, conceptualized geomechanical models of the critical dam sections, mechanical parameters of the rock mass and joint, as well as the physical modeling of the foundation stability were studied and are presented in the companion Part I paper (Figs. 1–4) [1]. However, considering the difficulties of simulating the effects of gradual degradation of

the shear strength of joints by physical model tests, to compensate the determination of the overall factor of safety of the dam sections, and to understand and estimate the uncertainties involved in physical model testing process [1], the numerical modeling approach was used to complete the stability study of the Three-Gorges Dam foundation. This Part II paper reports the results of the numerical modeling works, and discusses the overall evaluation of the stability of the Three-Gorges Dam foundation.

Under static loadings, the potential failure mechanisms that are normally investigated for a concrete dam foundation include four major modes: (i) sliding, (ii) deficient bearing capacity of foundation, (iii) non-uniform settlement, and (iv) uplift. In the case of the Three-Gorges Dam foundation, the geological

\*Corresponding author. Institute of Rock and Soil Mechanics, The Chinese Academy of Science, Xiaohongshan, Wuhan, Hubei 430071, China. Tel.: +86-27-871-97913; fax: +86-27-871-97386.

E-mail address: [jliu@dell.whrsm.ac.cn](mailto:jliu@dell.whrsm.ac.cn) (J. Liu).

Nomenclature			
$K$	factor of safety	$f_i$	friction coefficients of the assumed sliding surfaces of a rigid block in a limit equilibrium analysis
$\Sigma G$	total vertical load acting on the foundation surface of the dam	$c_i$	cohesion of the assumed sliding surfaces of rigid blocks in a limit equilibrium analysis
$G_z$	self-weight of the powerhouse	$l_i$	lengths of the assumed sliding surfaces of a rigid block in a limit equilibrium analysis
$P_1, P_2$	upstream and downstream horizontal loads acting on the dam structure, respectively	$\sigma_x, \sigma_y, \sigma_z$	normal stress components along $x, y, z$ axial directions, respectively
$\Sigma M$	total moment along the foundation surface of the dam	$f$	The friction coefficient
$\sigma'_n$	the vertical stress at the upstream starting point of the dam foundation surface	$c$	cohesion
$\sigma''_n$	the vertical stress at the downstream ending point of the dam foundation surface	$\phi$	friction angle
$B$	the width of the dam section	$\tau_n^{\max}$	the maximum shear stress of joints
$K_i$	the factor of safety against sliding of a specific rigid block in a limit equilibrium analysis, subscript $i$ is the number of rigid blocks	$\sigma_n$	normal stress across joints
$W_i$	vertical load acting on a rigid block in a limit equilibrium analysis	$k_s$	the shear stiffness of joints
$U_i$	uplift force acting on a rigid block in a limit equilibrium analysis	$k_n$	the normal stiffness of joints
$H_i$	horizontal force acting on a rigid block in a limit equilibrium analysis	$E$	elastic modulus of intact rock
$\alpha_i$	dip angle of an assumed sliding surface of a rigid block in a limit equilibrium analysis	$\nu$	Poisson's ratio of intact rock
$R_i$	horizontal resistant force between two adjacent rigid blocks in a limit equilibrium analysis	$\sigma_i$	mean value of normal stress components at Gauss points of a specific joint element in FEM
		$\tau_i$	mean value of shear stress components directing downstream along the joint surfaces at Gauss points of a specific joint element in FEM
		$A_i$	area of surface of a specific joint element in FEM



Fig. 1. Location of the Three-Gorges Project in China.

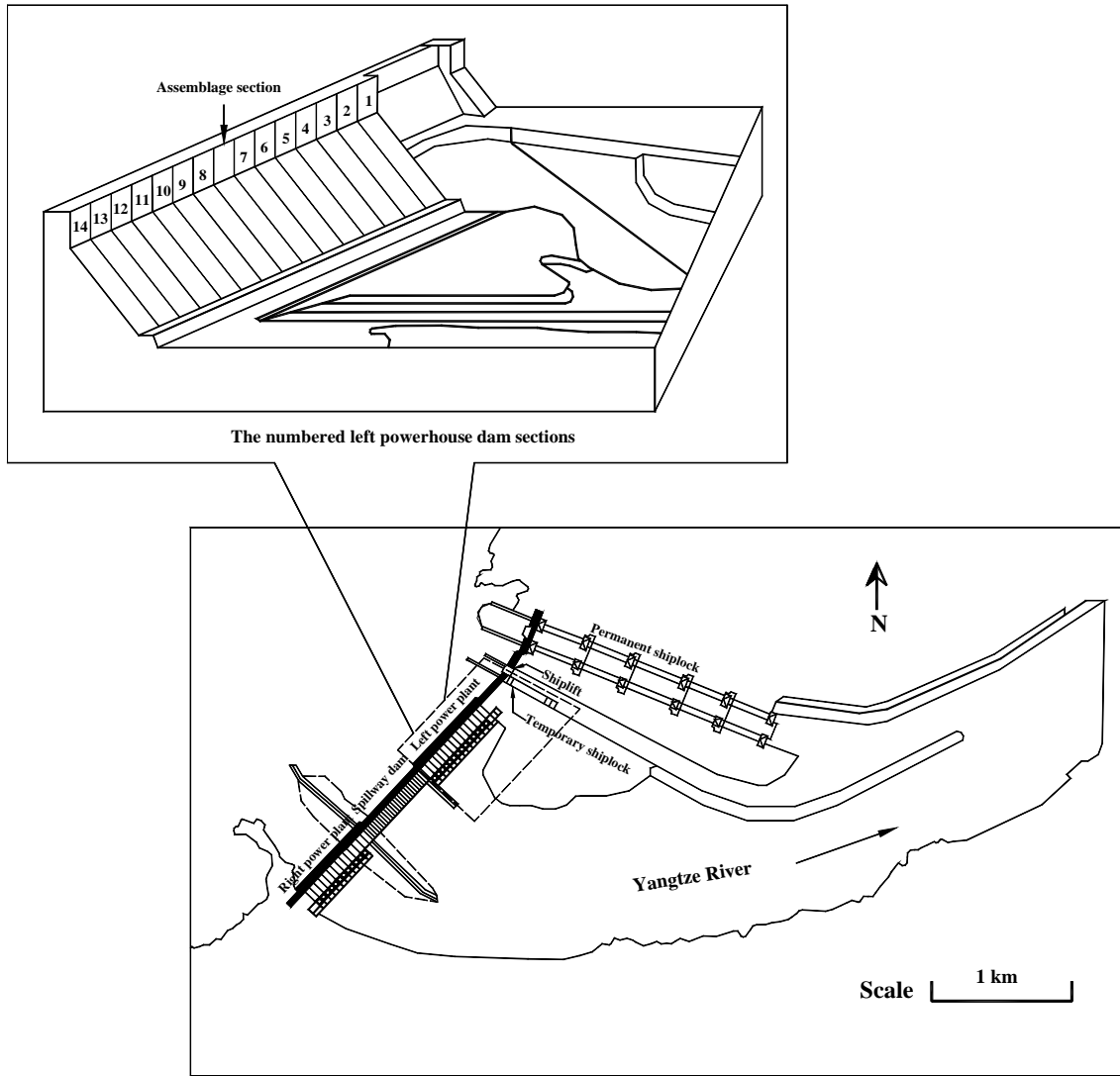


Fig. 2. Layout of the Three-Gorges Project and the numbered left powerhouse-dam sections.

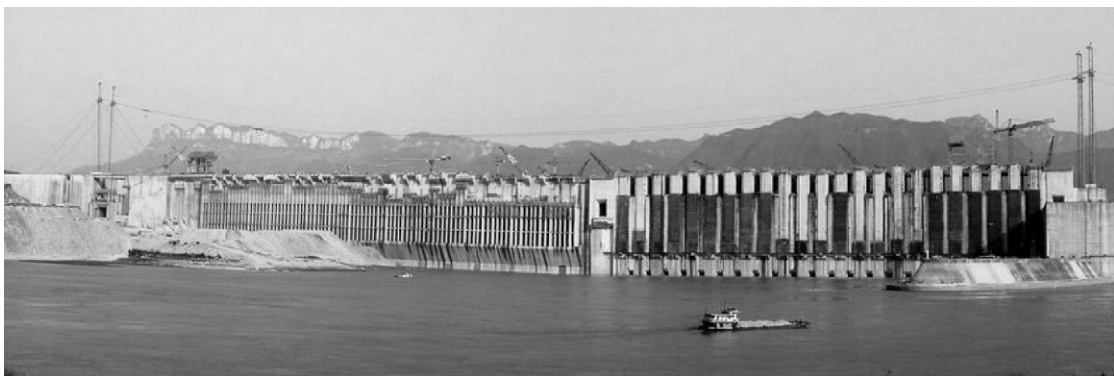


Fig. 3. Upstream view of the Three-Gorges Project under construction.

investigations, together with the laboratory and in situ tests for the properties of the rock mass, revealed that the dam foundation mainly comprises plagioclase granite that is intact, homogeneous, and of low

permeability and high strength. The faults and joints in the foundation have thin thickness with well-cemented tectonite. The joints are mostly not persistent, even in the regions where the gently dipping joints are

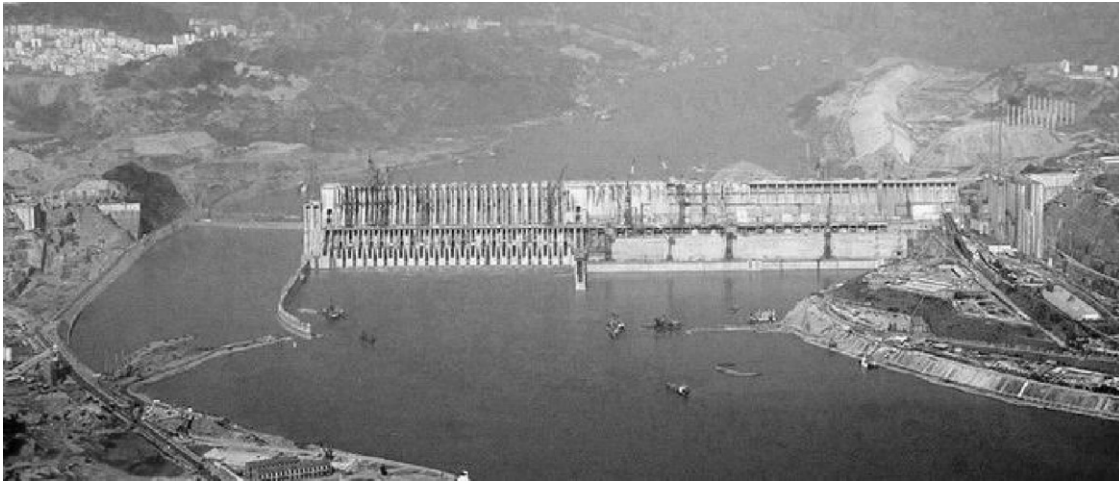


Fig. 4. Downstream view of the Three-Gorges Project under construction.

most developed: no deterministic and through-going sliding paths in the rock mass appear, due to the existence of the rock bridges [1]. For this reason, the other three modes could be excluded from these potential failure mechanisms, and thereby, the modeling works could focus on the stability against sliding along potential shearing paths comprised of gently dipping joints and intact rock bridges.

The sliding in a dam foundation is usually caused by two external factors: one is the overloading by the designed upstream hydrostatic load applied on a dam due to flooding; and the other is the gradual degradation of the shear strength of joints or other potential shearing paths due to water pressure, seepage, damage of joint surfaces, and geochemical reactions between water and joint surface minerals. Correspondingly, there should be two alternative definitions of the factor of safety as the index of stability. In the first case, the factor of safety is defined as the ratio between the maximum external load causing the sliding instability of the jointed rock mass and the designed load applied to the dam; while, in the second case, it is defined as the ratio between the comprehensive shear strength of joints and rock bridges along potential sliding paths and the mean shear stress required for limit equilibrium under the designed external loads [2]. To investigate the first sliding mode for the Three-Gorges Dam foundation, physical model tests were performed and proved to be an effective method (see Part I of this work [1]). However, it is difficult for the physical modeling techniques to consider the effects of the shear strength reduction of joints. Therefore, using numerical modeling to continue the stability study of the dam foundation is necessary. In the meantime, the numerical results can also be used to check the critical failure mechanism derived from the physical model tests.

Both the conceptualization of geomechanical conditions and the results of physical model tests have

demonstrated that the gently dipping joints are the most important factor governing the foundation stability, and the foundation of the no. 3 powerhouse-dam section is the most critical for the stability of the Three-Gorges Dam [1]. On the other hand, the foundation rocks are actually not cut into any complete blocks by the joints due to the existence of rock bridges; thus, the finite element method is more suitable than the distinct element method (DEM) or discontinuous deformation analyses (DDA) [3]. For this reason, this study, as Part II of the modeling works for the stability study of the Three-Gorges Dam, was performed using both limit equilibrium analyses and the finite element method (including both 2-D and 3-D analyses), based on the same geomechanical model as that used in physical model tests (see Figs. 5–8 and Table 1). The numerical modeling focuses on the stability conditions of the no. 3 dam section, but the constraint influences from the adjacent no. 2 and no. 4 sections are also included.

To identify the failure mechanism and derive the factor of safety, in the case of limit equilibrium analyses, the rock bridges were assumed as fictitious joints; the factor of safety was computed as the ratio between the resistant force and the driving force along a specific sliding path formed by both natural and fictitious joints. In the 2-D elasto-plastic FEM modeling, the friction coefficients and cohesions of the joints, rock bridges and foundation surfaces were decreased simultaneously and proportionally until the convergence could not be reached while the loading on the dam remains unchanged. The factor of safety is obtained as the ratio between the initial value and final decreased value of the shear strengths of the potential sliding paths. In the 3-D FEM modeling, the intact rock and concrete were modeled as elastic materials, while the joints and rock bridges were simulated as elasto-plastic media. The factor of safety was calculated as the ratio between the

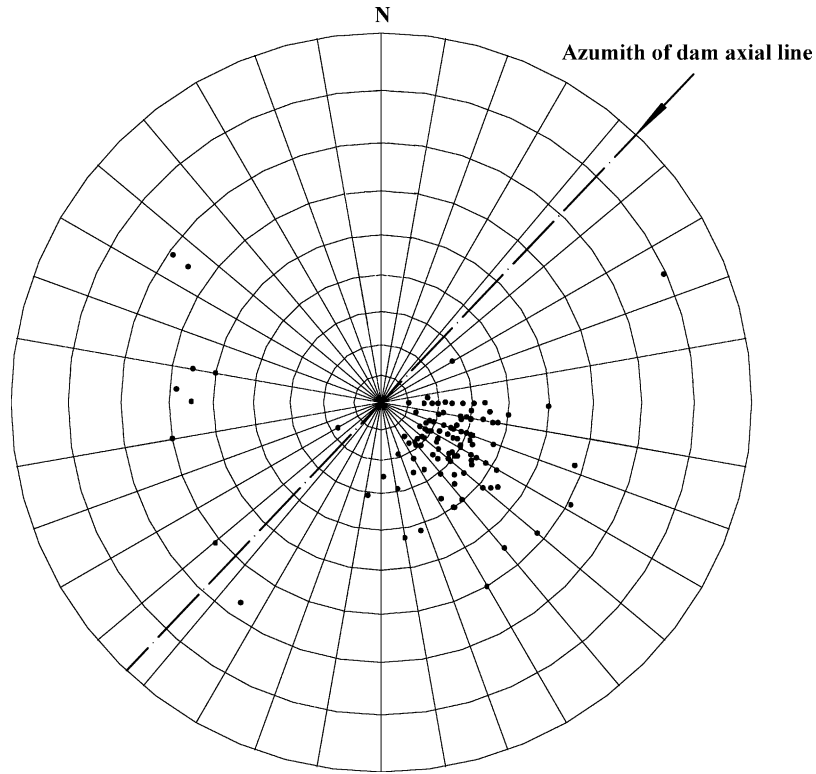


Fig. 5. Stereographic projection of the joints in the foundation of the most critical no. 3 powerhouse-dam section of the Three-Gorges Dam.

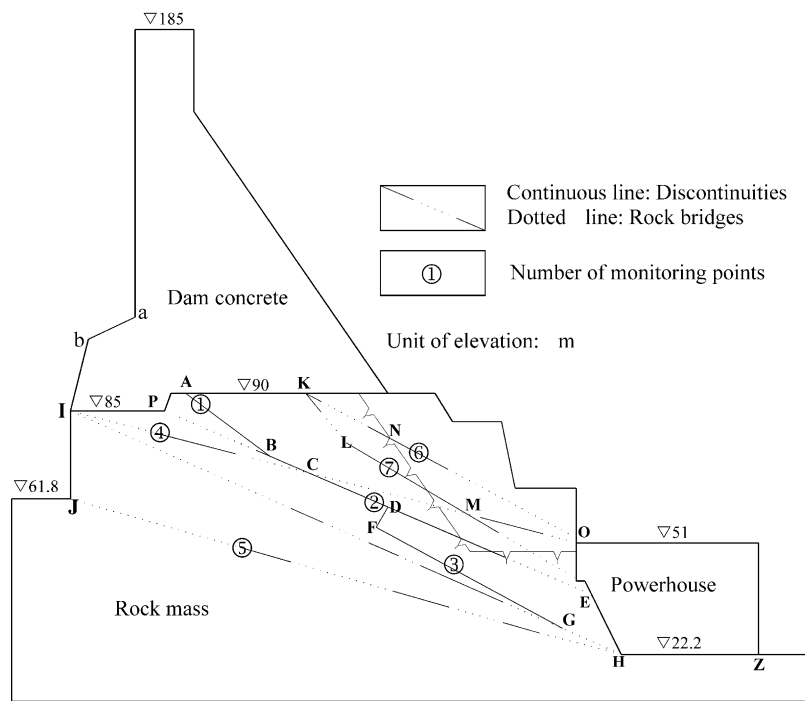


Fig. 6. Geological model of the no. 3 left powerhouse-dam section of the Three-Gorges Dam.

weighted mean of the shear strengths of all joint elements along potential sliding paths and the weighted mean of the shear stresses of these elements under the

designed load conditions. Following this, all the results derived from the different numerical models and the physical model tests are compared.

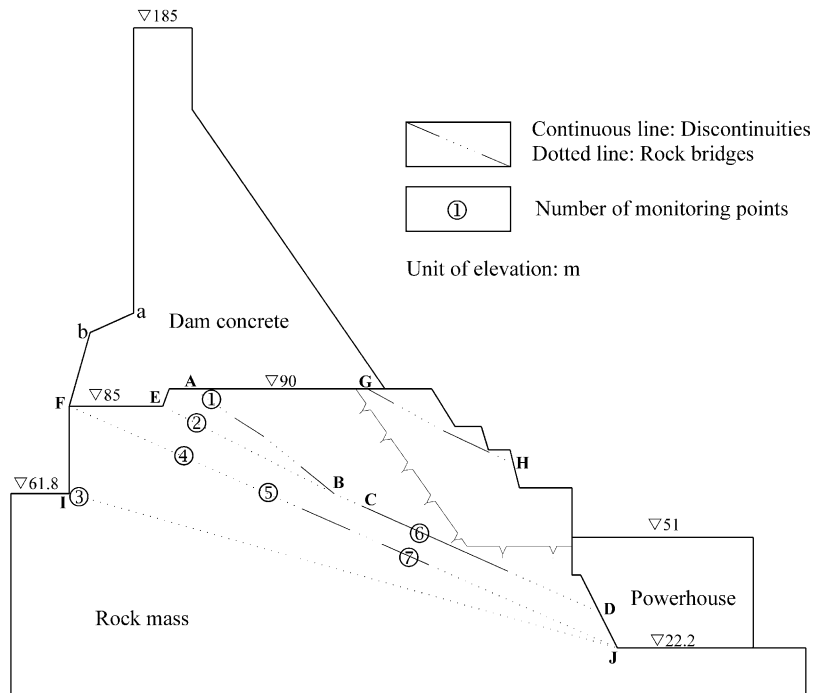


Fig. 7. Geological model of the no. 2 left powerhouse-dam section of the Three-Gorges Dam.

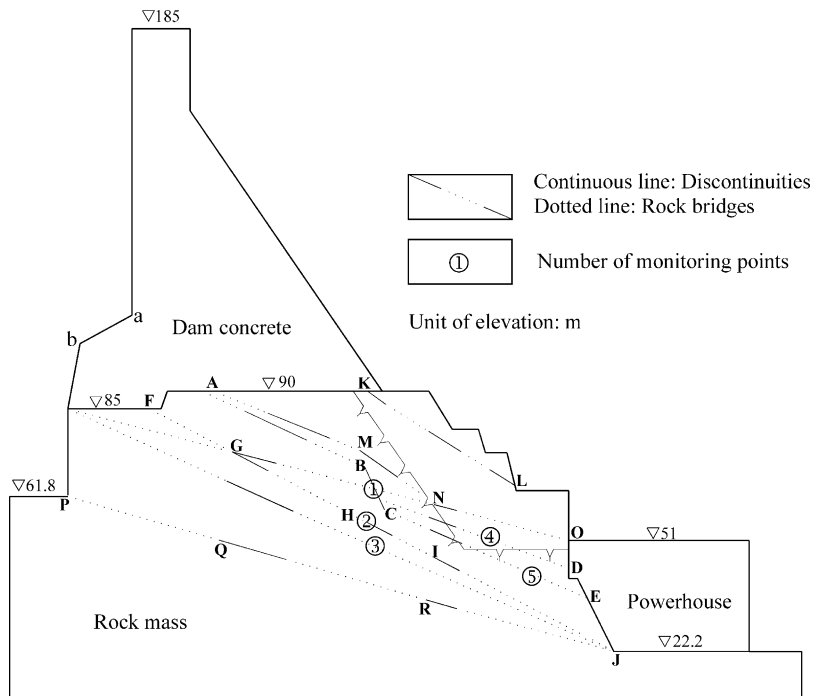


Fig. 8. Geological model of the no. 4 left powerhouse-dam section of the Three-Gorges Dam.

## 2. Limit equilibrium analyses

### 2.1. Methodology

In the limit equilibrium method, the rock mass is generally divided into a number of rigid blocks with

vertical fictitious interfaces, and the factor of safety is computed by establishing the static limit equilibrium conditions based on some assumed failure mechanisms [4,5]. This can be illustrated in Fig. 9 for an example of the assumed sliding path *ABCDFGHZ* in the foundation of the critical no. 3 powerhouse-dam section. In this

Table 1  
Mechanical parameters of the foundation rock and joint plane used in the stability studies

Type	Compressive strength (MPa)	Density (kN/m <sup>3</sup> )	Deformation moduli (GPa)	Poisson's ratio	Friction angle (deg)	Cohesion (MPa)
Plagioclase granite	100	27.0	35	0.20	59.6	2.0
Joint planes	—	—	—	—	35	0.2
Dam concrete	200	24.5	26	0.167	48	3.0
Foundation surface	—	—	—	—	48	1.3

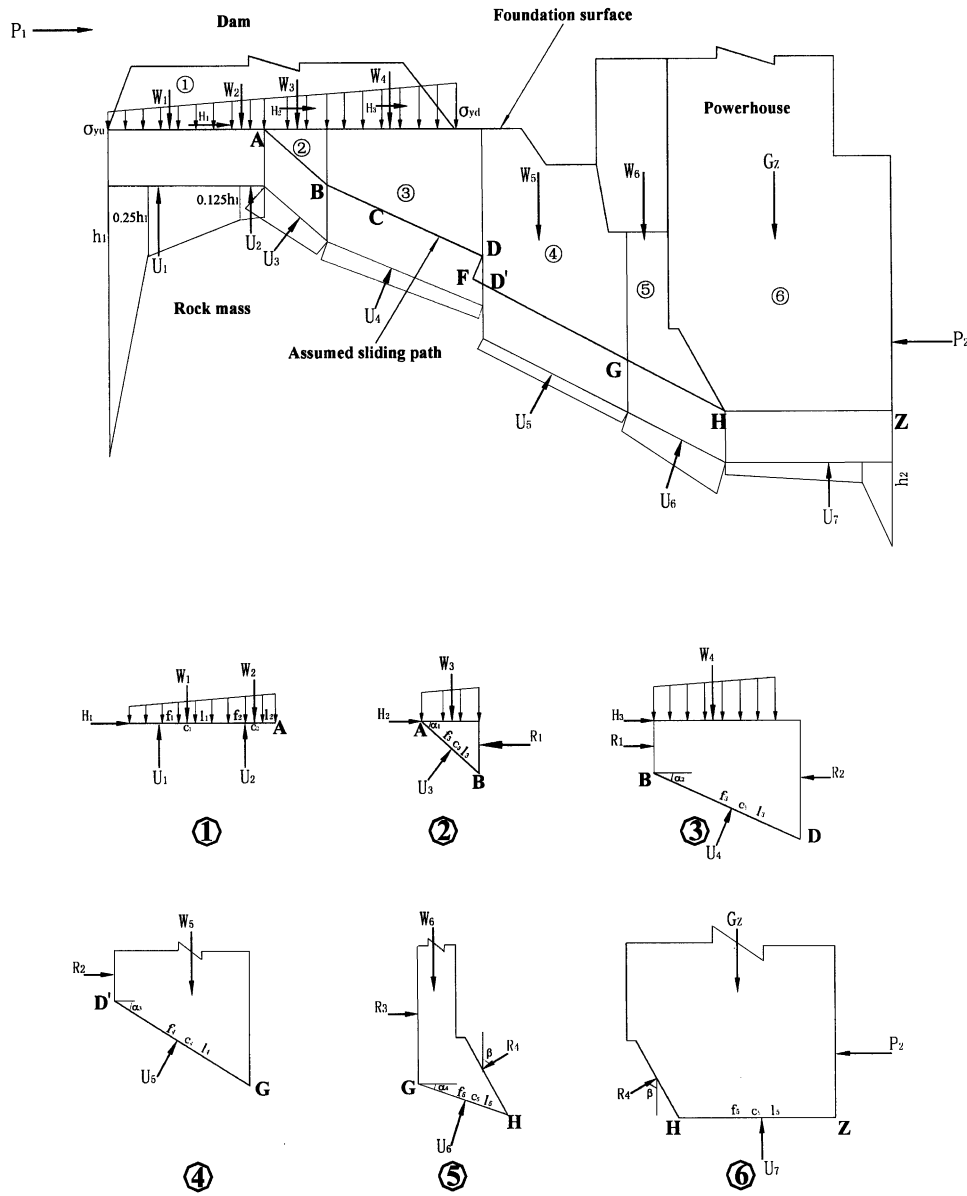


Fig. 9. Illustration of limit equilibrium analyses of the most critical sliding path *ABCDFGHZ* in the foundation of the no. 3 powerhouse-dam section of the Three-Gorges Dam.

analysis, the calculation of the factors of safety (*K*) along this specific sliding path can be determined through the following steps:

- (1) Calculation of the total vertical load  $\Sigma G$  acting on the foundation surface and the self-weight ( $G_z$ ) of the powerhouse.

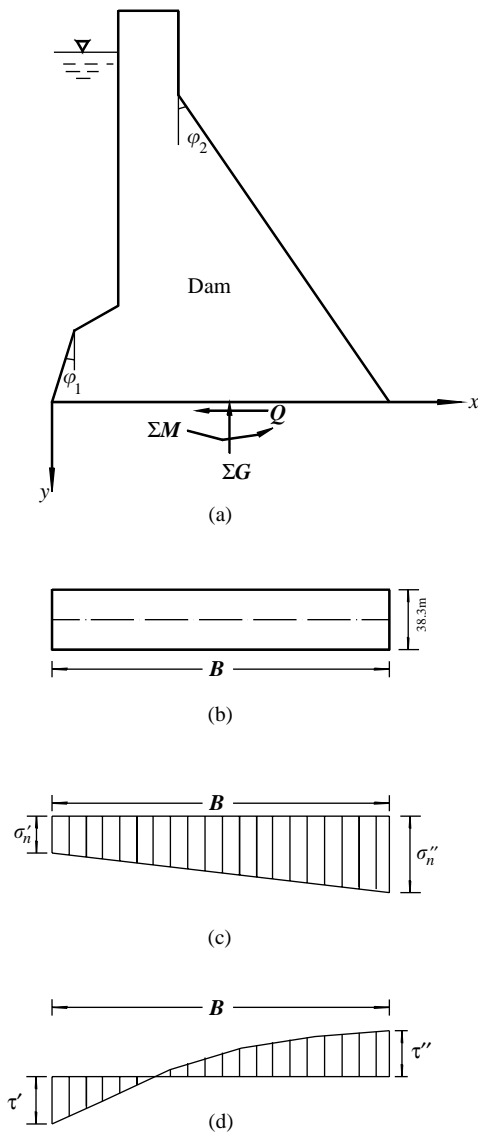


Fig. 10. Illustration of calculation of the vertical stress distribution along the foundation surface for limit equilibrium analyses: (a) cross section of dam section, (b) plan of foundation surface, (c) distribution of normal stresses along the foundation line, and (d) distribution of shear stresses along the foundation line.

- (2) Calculation of the total horizontal loads acting on the upstream surface ( $P_1$ ) and downstream surface ( $P_2$ ) of the dam structure, respectively.
- (3) Calculation of the vertical stress distribution along the foundation by using the Eqs. (1) and (2). The dam is eccentrically compressed and this distribution could be assumed as linear [6] (see Fig. 10).

$$\sigma'_n = \frac{\Sigma G}{B} - \frac{6\Sigma M}{B^2}, \quad (1)$$

$$\sigma''_n = \frac{\Sigma G}{B} + \frac{6\Sigma M}{B^2}, \quad (2)$$

where  $\sigma'_n$  and  $\sigma''_n$  represent the vertical stresses at the upstream starting point and downstream ending point of the foundation surface, respectively;  $\Sigma G$

represents the total vertical load acting on the foundation surface;  $\Sigma M$  is the total moment along the foundation surface; and  $B$  denotes the width of the dam section.

- (4) For the analyses, dividing the rock mass into six rigid blocks with vertical interfaces (see Fig. 9) according to the geometry of the assumed sliding path.
- (5) Calculation of the vertical loads  $W_i$  acting on the above six rigid blocks according to the vertical stress distributions along the foundation, as derived at Step 3.
- (6) According to limit equilibrium theory, if the shear forces along the fictitious interfaces between the rigid blocks are not considered, the factor of safety ( $K_i$ ) against sliding of each rigid block may be calculated by using the following equations:

$$K_1 = \frac{f_1(W_1 - U_1) + c_1l_1 + f_2(W_2 - U_2) + c_2l_2}{H_1}, \quad (3)$$

$$K_2 = \frac{f_3(W_3 \cos \alpha_1 - H_2 \sin \alpha_1 + R_1 \sin \alpha_1 - U_3) + c_3l_3}{W_3 \sin \alpha_1 + H_2 \cos \alpha_1 - R_1 \cos \alpha_1},$$

$$K_3 = \frac{f_3(W_4 \cos \alpha_2 - H_3 \sin \alpha_2 + R_2 \sin \alpha_2 - R_1 \sin \alpha_2 - U_4) + c_3l_4}{W_4 \sin \alpha_2 + H_3 \cos \alpha_2 - R_2 \cos \alpha_2 + R_1 \cos \alpha_2}, \quad (5)$$

$$K_4 = \frac{f_3(W_5 \cos \alpha_3 + R_3 \sin \alpha_3 - R_2 \sin \alpha_3 - U_5) + c_3l_5}{W_5 \sin \alpha_3 + R_2 \cos \alpha_3 - R_3 \cos \alpha_3}, \quad (6)$$

$$K_5 = \frac{f_3[W_6 \cos \alpha_4 - R_3 \sin \alpha_4 + R_4 \cos (\beta - \alpha_4) - U_6] + c_3l_6}{W_6 \sin \alpha_4 + R_3 \cos \alpha_4 - R_4 \sin (\beta - \alpha_4)}, \quad (7)$$

$$K_6 = \frac{f_4(G_p - R_4 \cos \beta - U_7) + c_4l_7}{R_4 \sin \beta - P_2}, \quad (8)$$

where  $W_1, W_2, W_3, W_4, W_5, W_6$  are the vertical loads, and  $U_1, U_2, U_3, U_4, U_5, U_6, U_7$  are the uplift forces acting on the no. 1–6 rigid blocks, respectively;  $G_z$  represents the weight of the powerhouse.  $P_1$  is the total horizontal load acting on the upstream surface of the dam structure;  $P_2$  is the total horizontal load acting on the downstream surface of the dam structure;  $H_1, H_2, H_3$  are the horizontal forces distributed on the no. 1–3 rigid blocks, respectively;  $\alpha_1, \alpha_2, \alpha_3, \alpha_4$  denote the dip angles of the assumed sliding surface of the rigid blocks;  $R_1, R_2, R_3, R_4$  are the horizontal resistant forces between two adjacent rigid blocks;  $\beta$  is the intersection angle between the vertical direction and  $R_4$ ;  $f_1, f_2, f_3, f_4$  are the friction coefficients of the assumed sliding surfaces of the rigid blocks, which is derived as the weighted means of those of both the joints and rock bridges.  $c_1, c_2, c_3, c_4$  are the cohesions of the assumed sliding surfaces of the rigid blocks, which are also derived as the weighted

Table 2

Safety factors of the typical sliding paths of no. 3 left powerhouse-dam section of the Three-Gorges Dam calculated by limit equilibrium methods

Sliding paths	<i>ABCDE</i>	<i>PBCDE</i>	<i>ABCDFGH</i>	<i>ABCDFGHZ*</i>	<i>KNO</i>	<i>KLME</i>	<i>IH</i>	<i>JH</i>	<i>ICDE</i>
Safety factors	3.21	3.37	3.08	4.17*	3.85	3.99	3.82	5.15	4.99

Note: Asterisk denotes that the safety factor was computed when the powerhouse effects were considered; If there is no asterisk, the safety factor was computed when the powerhouse effects were not considered.

means of those of both the joints and rock bridges.  $l_1, l_2, l_3, l_4$  are the lengths of the assumed sliding surfaces of the rigid blocks.

Only if all the divided rigid blocks reach the limit force-equilibrium state simultaneously, can the sliding along the assumed sliding path *ABCDFGH* happen. In other words, when the sliding occurs, the factors of safety of all the rigid blocks equal each other. This can be described in Eq. (9).

$$K_1 = K_2 = K_3 = K_4 = K_5 = K_6 = K. \quad (9)$$

In addition, there is the following relationship to be used for the calculation:

$$P_1 = H_1 + H_2 + H_3 \quad (10)$$

and

$$H_2 = \frac{\tau_2}{\tau_2 + \tau_3}(P_1 - H_1), \quad (11)$$

$$H_3 = \frac{\tau_3}{\tau_2 + \tau_3}(P_1 - H_1), \quad (12)$$

where  $\tau_2, \tau_3$  are the mean shear stresses along the foundation surface distributed on the no. 2 and no. 3 rigid blocks.

Finally, by substituting Eqs. (9)–(12) into Eq. (3)–(8) and solving these substituted equations by iteration, we could derive the factor of safety *K*.

### 2.2. Results of limit equilibrium analyses

The factors of safety were derived for all the potential sliding paths of the no. 3 powerhouse-dam section by using the above methodology. As shown in Table 2, when the powerhouse effect, (which is defined as the resistant effect against sliding provided by integrating the powerhouse with the dam body through downstream slope surface, see Fig. 6) was not taken into account, the factor of safety of sliding path *ABCDFGH* is 3.08, the lowest among all these assumed sliding paths. Since the foundation stability would be governed by the sliding path with the lowest factor of safety, when the powerhouse effects were not taken into account, this lowest factor of safety can be defined as the factor of safety of the dam foundation. However, the factor of safety of sliding path *ABCDFGHZ* in the foundation of the no. 3 dam section is 4.17 when the powerhouse effects are considered (see Table 2). Note that the above factor of safety derived should be considered as conservative because the full uplift forces along the

assumed sliding paths were taken into account. In fact, the uplift forces should be low due to the existence of the rock bridges.

### 3. Finite element analyses

In the finite element analyses, 2-D numerical modeling was firstly conducted and focused on the stability conditions of the most critical no. 3 powerhouse-dam section. Then, 3-D numerical modeling was performed to study the constraint influences on the no. 3 section from the adjacent no. 2 and no. 4 powerhouse-dam sections.

#### 3.1. 2-D numerical modeling of the single no. 3 powerhouse-dam section

2-D numerical modeling was performed to analyze the foundation stability of the no. 3 powerhouse-dam section, using an elasto-plastic FEM approach. The behaviors of rock and concrete were simulated by use of linear solid isoparametric elements, and the behaviors of rock bridges, joints and foundation surfaces were modeled using quadratic joint elements. The mechanical parameters of the rock, joints, foundation surfaces, as well as concretes used in this numerical modeling, are the same as those adopted in the physical modeling (see Table 1).

Considering the Drucker–Prager failure criterion yields a smooth failure surface and is quite convenient for finite element analyses [7,8], it was adopted as the plastic potential for the intact rock blocks and concrete structure, which can be represented as

$$F = \alpha I_1 + \sqrt{J_2} - \omega = 0, \quad (13)$$

where

$$I_1 = \sigma_x + \sigma_y + \sigma_z, \quad (14)$$

$$J_2 = \frac{1}{6}[(\sigma_x - \sigma_y)^2 + (\sigma_y - \sigma_z)^2 + (\sigma_x - \sigma_z)^2 + 6(\tau_{xy}^2 + \tau_{yz}^2 + \tau_{zx}^2)], \quad (15)$$

$$\alpha = \frac{f}{(9 + 12f^2)^{1/2}}, \quad (16)$$

$$\omega = \frac{3c}{(9 + 12f^2)^{1/2}}, \quad (17)$$

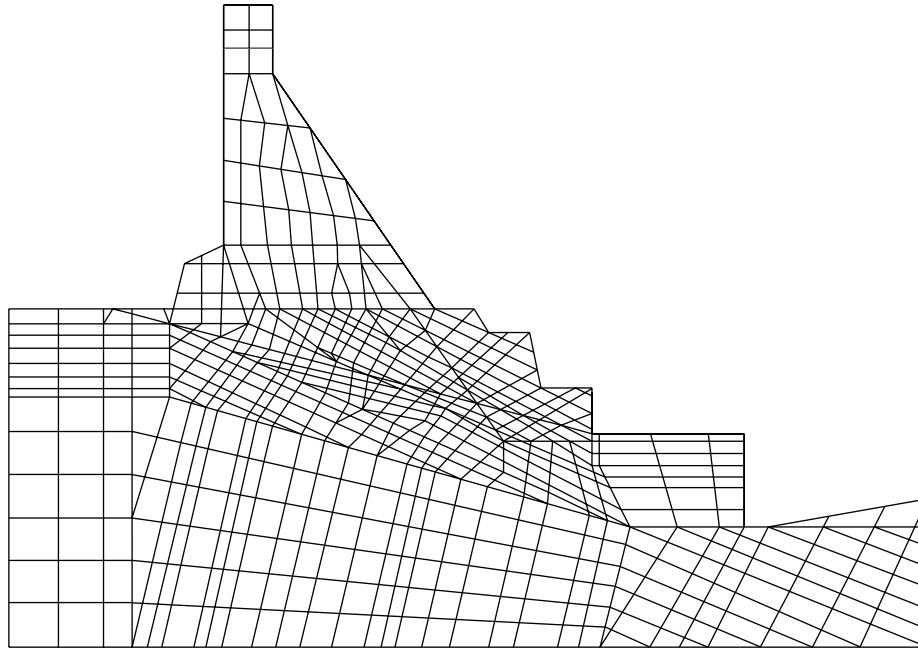


Fig. 11. 2-D FEM mesh for the stability analyses of the no. 3 powerhouse-dam section.

Among them,  $\sigma_x$ ,  $\sigma_y$ ,  $\sigma_z$  are the normal stress components, respectively, in the  $x$ ,  $y$ ,  $z$  directions;  $f$  is the friction coefficient; and  $c$  is the cohesion value of the intact rock.

The Mohr–Coulomb criterion was considered as the failure criterion of joint elements, which can be represented as

$$\tau_n^{\max} = c - \sigma_n \tan \phi, \quad (18)$$

where  $\tau_n^{\max}$ ,  $\sigma_n$  and  $\phi$ , respectively, represent the maximum shear stress, normal stress and friction angle of the joints. The shear stiffness and normal stiffness of joints are determined by the slopes of the stress–strain curves in laboratory tests [9–12]. The shear stiffness  $k_s$  and normal stiffness  $k_n$  of rock bridges are calculated using the mechanical properties of intact rocks, according to the following Eqs. (19) and (20) [13,14]:

$$k_s = G = \frac{E}{2(1 + \nu)}, \quad (19)$$

$$k_n = k + \frac{3}{4}G, \quad (20)$$

where

$$k = \frac{E}{3(1 - 2\nu)}. \quad (21)$$

The symbol  $G$  is the shear modulus,  $E$  the elastic modulus and  $\nu$  the Poisson's ratio.

The computational model of the dam foundation has a size of 160 m in depth, 95 m in length directing upstream from the dam heel and 220 m in length directing downstream from the dam toe. For the

boundary conditions, the normal displacement constraints were applied to the upstream and downstream boundaries of the numerical model, while a fixed displacement constraint is applied to the bottom boundary. Note that this 2-D modeling was considered as plane strain conditions and the constraint effects induced by the adjacent foundations of the no. 2 and no. 4 powerhouse-dam sections are ignored. The FEM mesh for the no. 3 section model is illustrated in Fig. 11.

To investigate the failure mechanism and determine the factor of safety of this dam section, the numerical computation was carried out in the following steps. In the first step, the self-weights of the rock mass and concrete structure were considered. Then, the normal external load combination, including the upstream hydrostatic load, was applied in five increment steps, each being considered as 20% of the total. Afterwards, while keeping the applied load conditions unchanged, the values of shear strengths of the joints, rock bridges and foundation surfaces, including friction coefficient ( $f$ ), cohesion ( $c$ ), shear stiffness ( $k_s$ ) as well as normal stiffness ( $k_n$ ), were simultaneously and progressively decreased according to an identical percentage. Meanwhile, to examine the detailed development process of the yielding zones and failure occurrences, these identical percentages were defined within a range of less than 10% of the initial parameter values. The computation continued until a divergence occurs. This divergence of numerical modeling may be regarded as the losing of static force-equilibrium state and thus could be taken as the failure conditions. Consequently, the factor of safety of the dam is generally defined as the ratio

Table 3  
Displacements of key points of no. 3 dam section under normal loading combination derived from the 2-D numerical modeling

Displacements of dam top (mm)		Displacements of dam heel (mm)		Displacements of dam toe (mm)	
Horizontal	Vertical	Horizontal	Vertical	Horizontal	Vertical
10.94	−8.32	1.76	−0.55	1.63	−5.23

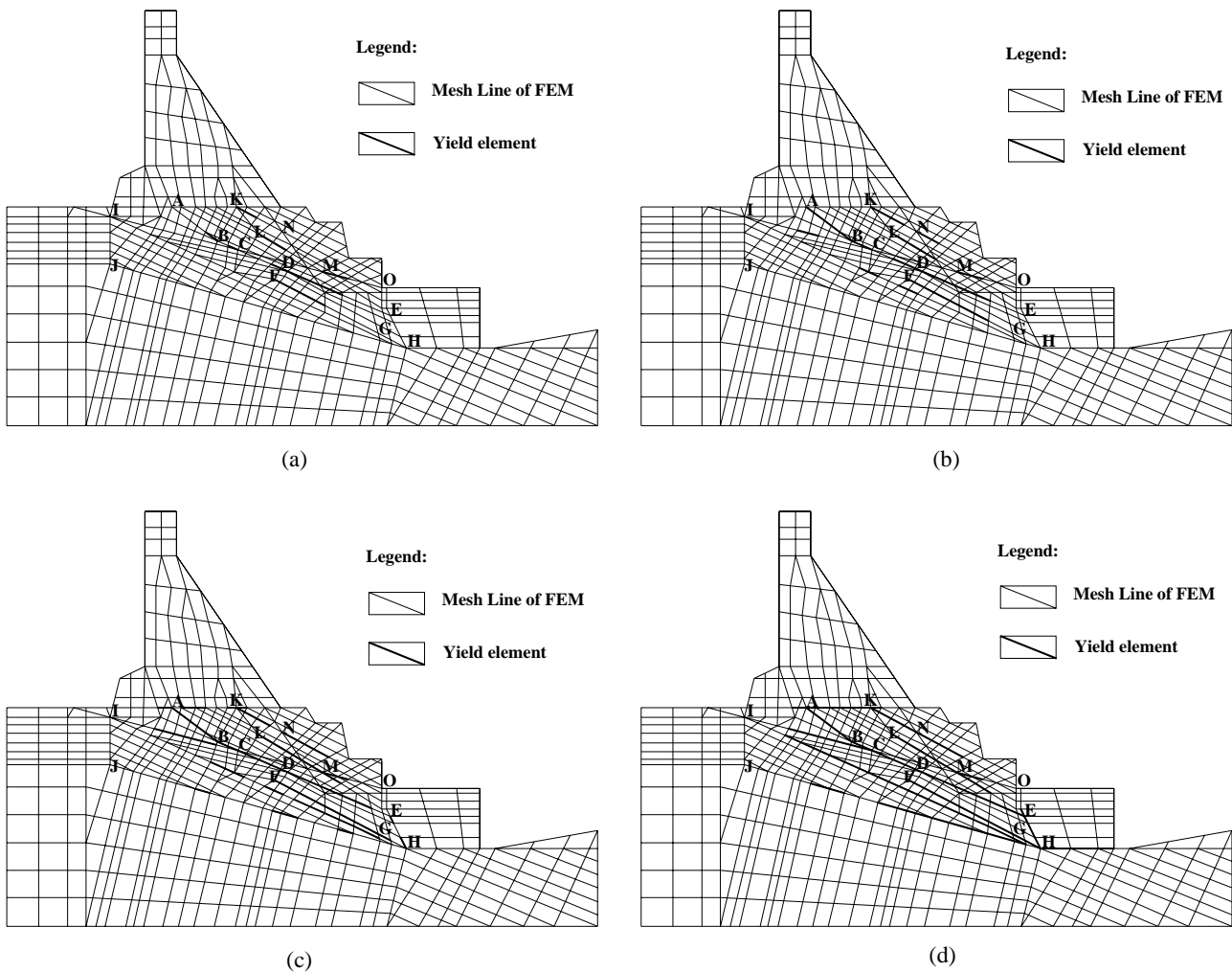


Fig. 12. Development of yielding elements due to the gradual reduction of the shear strengths of assumed sliding paths derived from 2-D finite element analyses of the no. 3 powerhouse-dam section of the Three-Gorges Dam. Distribution of yielding elements when friction coefficient ( $f$ ), cohesion ( $c$ ), shear stiffness ( $k_s$ ) and normal stiffness ( $k_n$ ) along the assumed sliding paths are simultaneously decreased by (a) 80%, (b) 60%, (c) 40%, and (d) 26% of their initial values.

between the initial values and final decreased values of the shear strengths of the potential sliding paths.

As shown in Table 3, the numerical results show that under the normal loading combination and initial shear strength values, the horizontal displacements at the dam heel and toe are both less than 2.0 mm. Besides, there are not any yielding zones occurring in the simulated domain. This reveals that for this designed normal loading combination and initial strength values, the

foundation of the no. 3 powerhouse-dam section is stable.

Fig. 12 illustrates several typical stages of the yielding element development in the simulated domain following the gradual decrease of the initial shear strength values during the computing process. When the initial values of  $f$ ,  $c$ ,  $k_s$ ,  $k_n$  of the joints and rock bridges were simultaneously decreased by 26%, the yielding zones were developed through the

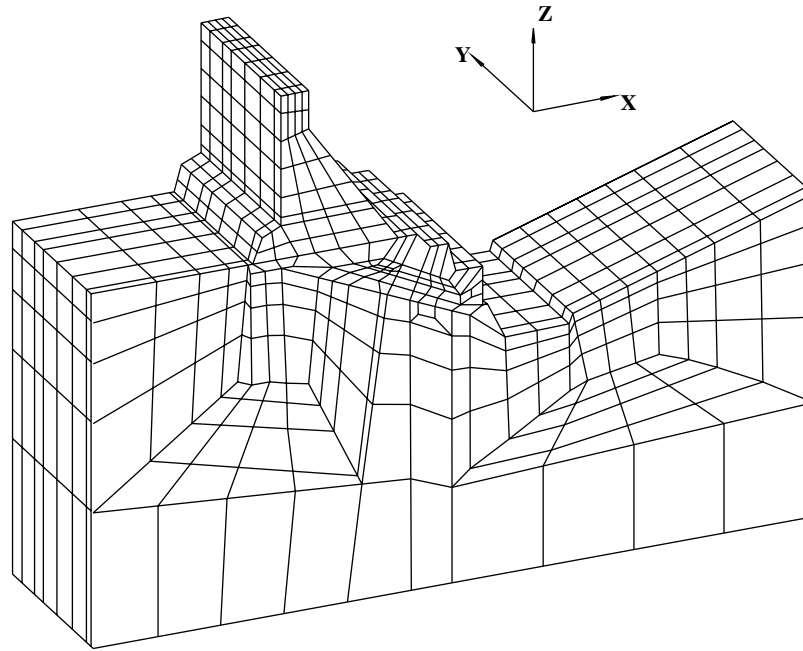


Fig. 13. 3-D FEM mesh for the stability analyses of the combined no. 2, 3, 4 powerhouse-dam sections.

Table 4

Displacements of key points of no. 3 dam section under normal loading combination derived from the 3-D numerical modeling

Displacements of dam top (mm)		Displacements of dam heel (mm)		Displacements of dam toe (mm)	
Horizontal	Vertical	Horizontal	Vertical	Horizontal	Vertical
3.85	-7.81	1.62	-4.35	1.52	-4.65

sliding paths of *ABCDFGH*, and then *ABCDEH*. Many other joint elements also behave plastically. Subsequently, convergence cannot be reached. It was therefore concluded that starting at this moment, the static force-equilibrium along the potential sliding path of *ABCDFGHZ* was lost and dam sliding would happen. The factor of safety was calculated as 3.85.

### 3.2. 3-D numerical modeling of associated no. 2, 3, 4 powerhouse-dam sections

The factor of safety of the no. 3 powerhouse-dam section derived from the above 2-D numerical modeling may be regarded as over-conservative since the constraint effects on the stability of the no. 3 section by its adjacent no. 2 and no. 4 sections were not taken into account. This is the main reason and objective of the 3-D FEM modeling.

The domain of this 3-D FEM model included the three dam sections, powerhouse basements and dam foundations, with a model size of 205 m in depth, 114.9 m in width (the same as the total width of the three

dam sections), 109.5 m in length directing upstream from the dam heel and 311.5 m in length directing downstream from the dam toe, respectively. For the boundary conditions, the normal displacement constraints were applied to the upstream and downstream boundaries of the model, while a fixed displacement constraint was applied to the bottom boundary. The left and right sides were left as free surfaces. Fig. 13 depicts the 3-D model mesh.

Similar to the 2-D numerical modeling, 3-D linear solid isoparametric elements were used to simulate the rock and dam body while quadratic solid joint elements were adopted to model the joints and rock bridges. The Drucker–Prager and Mohr–Coulomb criteria were considered as the failure criteria for the above two types of the elements. The input mechanical parameter values and the normal load combination were the same as those used in the 2-D numerical modeling. In terms of the computational steps, self-weights of the rock mass and concrete structures were loaded first, and then the normal external loads were applied.

For the 3-D calculations, the overall factor of safety *K* along a specific sliding path was calculated by the

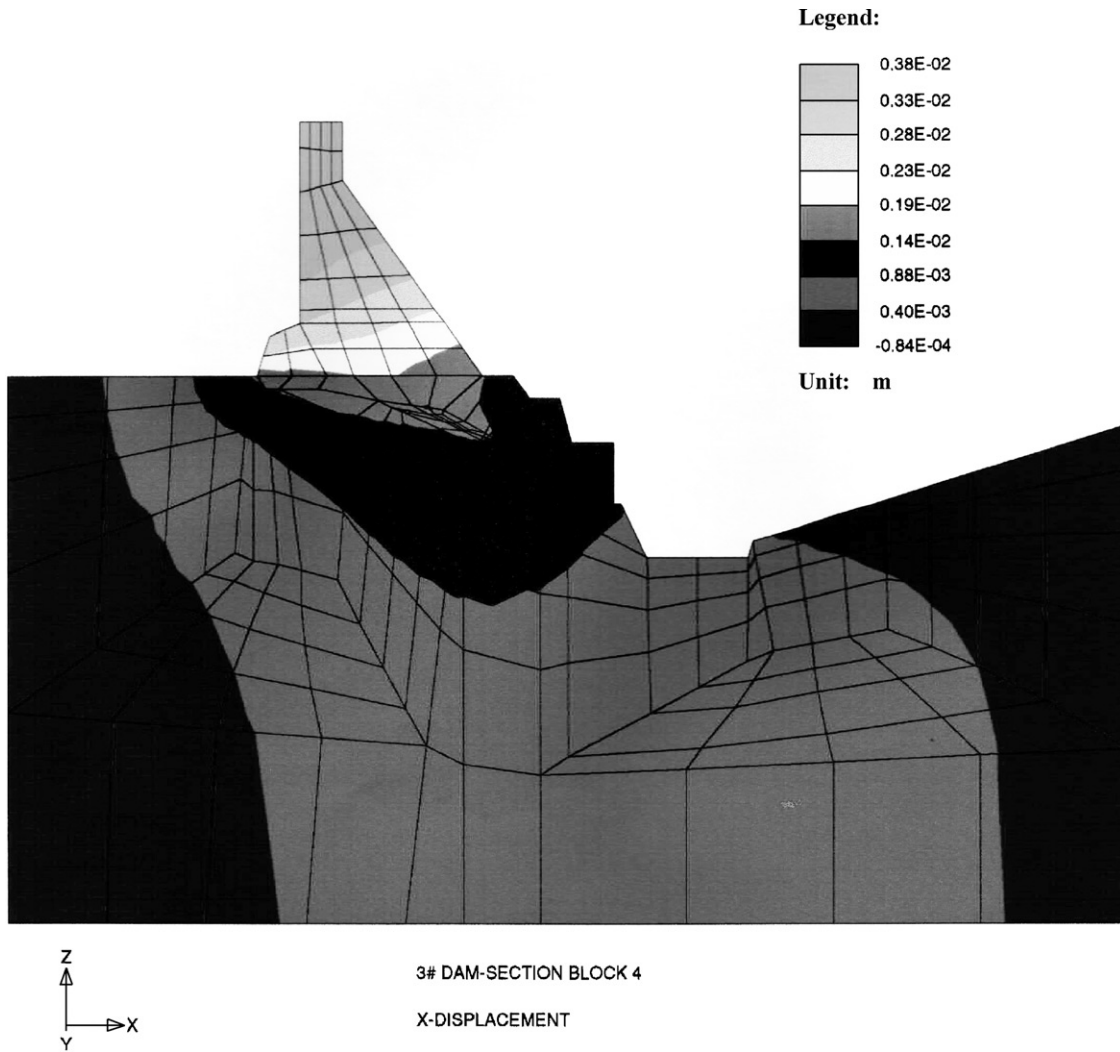


Fig. 14. Distributions of horizontal displacements of the dam center-line section of the no. 3 powerhouse-dam section derived from 3-D FEM.

following equation:

$$K = \frac{\sum f \sigma_i A_i + \sum C A_i}{\sum \tau_i A_i}, \quad (22)$$

where  $\sigma_i$  is the mean value of the normal stress components at the Gauss points of a specific joint (or rock bridge) element;  $\tau_i$  is the mean value of shear stress components directing downstream along the joint surfaces at the Gauss points;  $A_i$  represents the area of the surface of a specific joint element; and subscript  $i$  denotes the numbers of the joint/bridge element of the potential sliding paths.

Eq. (22) represents the limit equilibrium state between the shear force and shear strength along a potential sliding path. As such, this definition of factor of safety reflects the margin of the shear strengths against sliding along the specific sliding path, similar to that used in the 2-D numerical modeling.

As shown in Table 4, the 3-D numerical results show that under the normal loading combination, the horizontal displacements at the dam heel and toe are both less than 2.0 mm. Figs. 14 and 15 illustrate the distributions of horizontal and vertical displacements of the dam, in a center-line section of the no. 3 powerhouse-dam section; Figs. 16 and 17 give the distributions of maximum and minimum principal stresses in the same section.

The factors of safety along some critical potential sliding paths have been computed by using Eq. (22). The comparisons between them demonstrated that the potential sliding paths with the lowest factors of safety are, respectively, ABCDFGH for no. 3 dam section, ABCD for no. 2 dam section and ABCD for no. 4 dam section (see the geological models as illustrated in Figs. 6–8). Table 5 lists these lowest factors of safety and the corresponding potential sliding paths. The factor of safety of the no. 3 dam section is less than that of the no. 2 and no. 4 dam sections, demonstrating that the

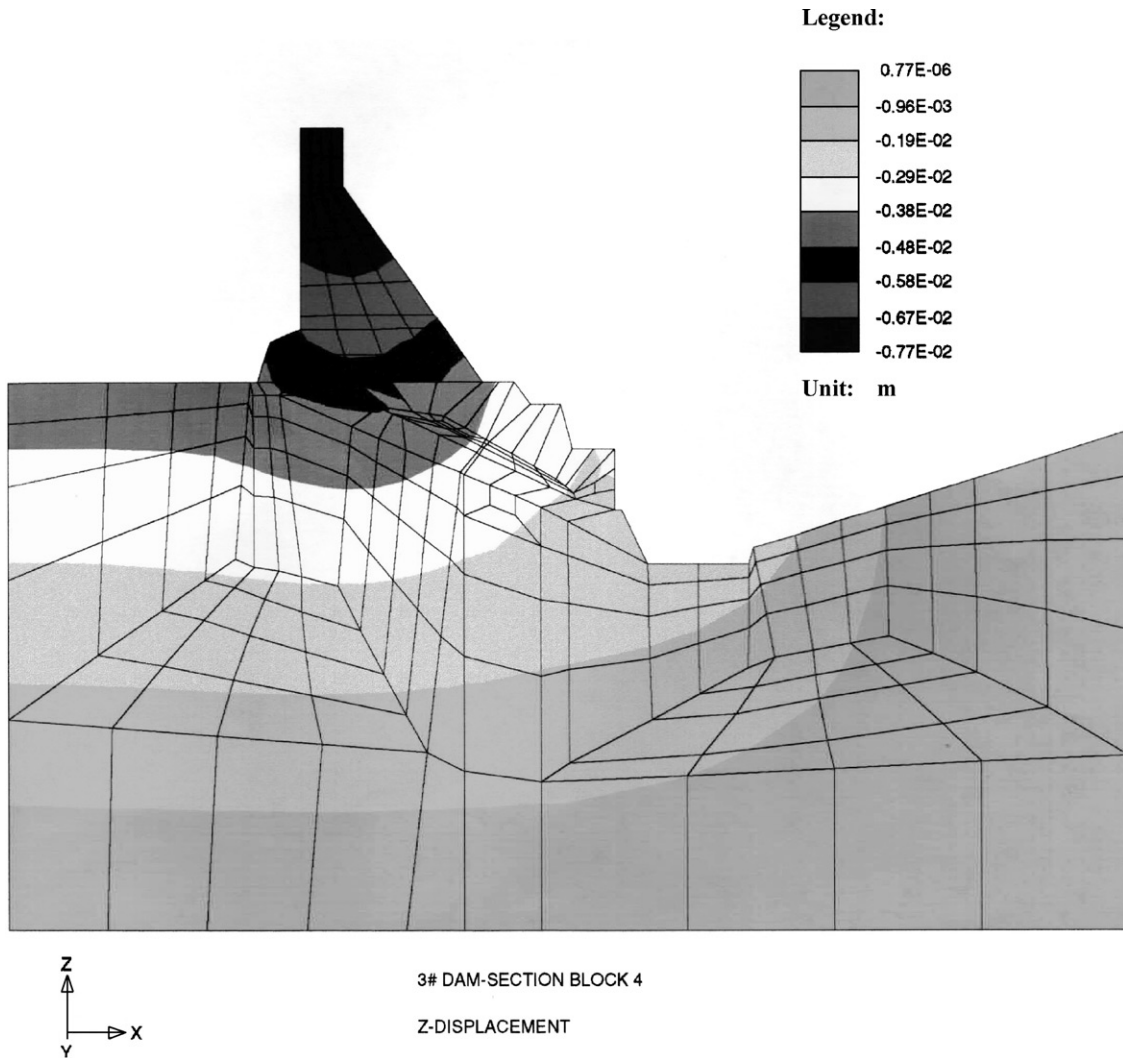


Fig. 15. Distributions of vertical displacements of the dam center-line section of the no. 3 powerhouse-dam section derived from 3-D FEM.

stability of the no. 3 section is poorest among the dam sections and the constraint effects induced by the adjacent no. 2 and no. 4 dam sections are important to the foundation stability of the no. 3 dam section. The lowest value of the factor of safety for no. 3 section is 4.37.

#### 4. Comparisons and discussions

In total, two physical model tests (the 2-D and 3-D physical model tests) and three computational modeling (the limit equilibrium analyses, 2-D and 3-D finite element analyses) have been carried out. Altogether, these studies mainly focused on the foundation stability of the most critical no. 3 powerhouse-dam section and a common geomechanical model was used. The results from these different approaches are compared and discussed below.

##### 4.1. Displacements

Table 6 compares the experimental and FEM results of the horizontal and vertical displacements at dam top, heel, and toe of the no. 3 powerhouse-dam section. For both 2-D and 3-D cases, the experimental results of displacements agree fairly well with the FEM results under the same normal loading conditions. Both the experimental and FEM results reveal that horizontal displacements downstream, in general, agree well with magnitude values of 2.0 mm or smaller at the dam heel and toe. There are two major reasons for this. One is because the geomechanical model, initial and loading conditions, and boundary conditions used for the 2-D/3-D physical model test and FEM are identical; another lies in the fact that the system behaves elastically in general and the plastic deformations of intact rocks and concrete have not happened under the normal loading combination.

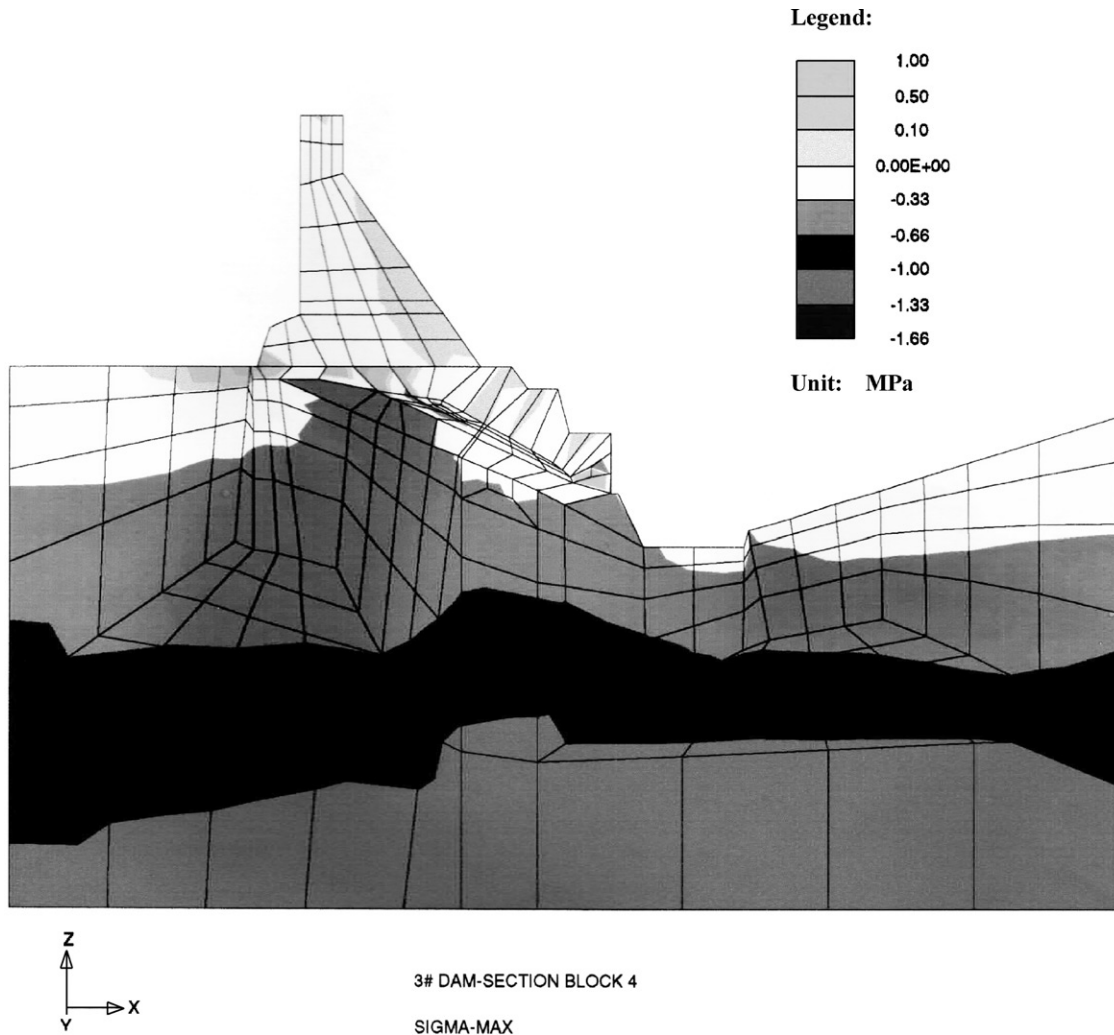


Fig. 16. Distributions of maximum principal stresses of the dam center-line section of the no. 3 powerhouse-dam section derived from 3-D FEM.

On the other hand, the horizontal and vertical displacements at the dam top, heel, and toe obtained from the 2-D modeling (for both physical model tests and FEM modeling) are larger as compared to the 3-D results. It is mainly because of the more conservative natures of the 2-D models compared to the 3-D ones, with the main differences being in the boundary conditions. In the 2-D cases, the left and right sides of the foundation of the no. 3 powerhouse-dam section were modeled as the free surfaces; while, in the 3-D cases, the constraint effects applied by the adjacent no. 2 and no. 4 dam sections were included, thus resulting in the smaller deformations and improved stability of the no. 3 dam section.

4.2. Failure mechanisms

As aforementioned, both the numerical simulations and physical model tests demonstrate that under normal loading conditions, the foundation

and concrete structure of the no. 3 powerhouse-dam section behave elastically. Both physical and numerical models indicated that the path *ABCDFGH* is the most critical potential sliding path and plays a dominant role in the foundation stability for the no. 3 section. In both the 2-D and 3-D physical model tests, this dominant sliding path extends into *aA* and *bA* paths (see Part I of this paper [1]) of the dam body, and thus suggest that the strengths of the concrete structure play a positive role in the stability against sliding (refer to Fig. 18). However, in the numerical analyses, this critical sliding path connects with the foundation surfaces, which was assumed as a part of this potential sliding path in the computations. In the physical model test, the slide paths and failure of the dam were obtained without such assumptions during the process of loading when the similarity requirements were met in advance. This can be regarded as the limitations of the numerical modeling approaches.

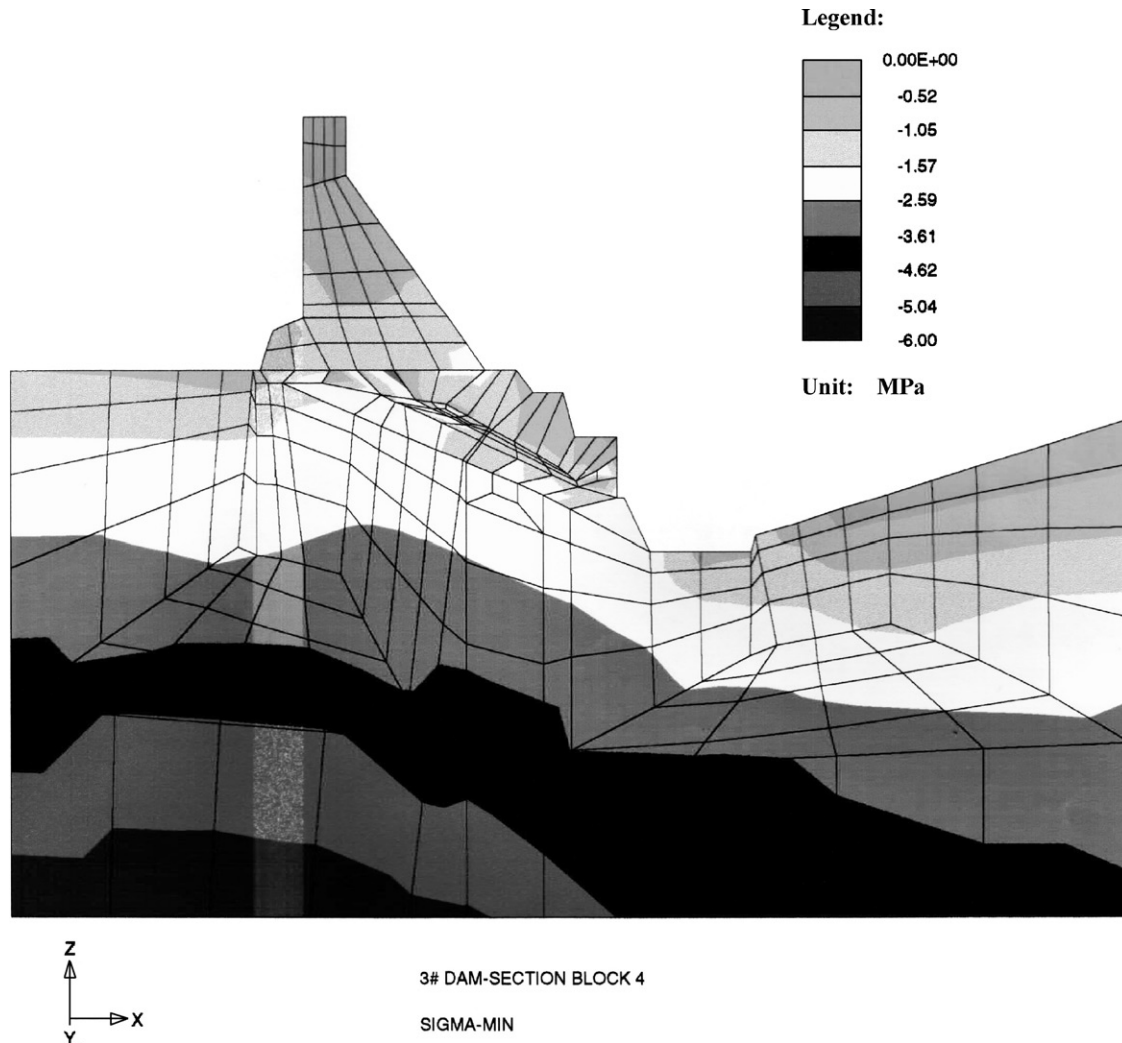


Fig. 17. Distributions of minimum principal stresses of the dam center-line section of the no. 3 powerhouse-dam section derived from 3-D FEM.

Table 5  
Safety factors of the most critical sliding paths of no. 2, 3, 4 left powerhouse-dam section of the Three-Gorges Dam calculated by 3-D FEM

Dam sections	Most critical sliding paths	Safety factors
No. 2 dam section	<i>ABCD</i>	5.88
No. 3 dam section	<i>ABCDFGH</i>	4.37
No. 4 dam section	<i>ABCD</i>	5.53

#### 4.3. Factor of safety

Table 7 shows the agreements and discrepancies in the factors of safety of the no. 3 powerhouse-dam section derived from the diverse approaches. When the powerhouse effects are taken into account, the factor of safety from the 2-D physical model test and FEM are 3.5 and 3.85, respectively, both being lower as compared to the

3-D experimental and FEM results, which are 4.0 and 4.37, respectively. In addition, the factor of safety computed by the limit equilibrium method is 3.08/4.17 whether the effects of powerhouse are taken into account or not.

There may be four major reasons for the discrepancies.

- The difference between the factors of safety from the 2-D and 3-D physical/numerical modeling are mainly resulting from the different boundary conditions, which are the assumed free surface conditions for the left and right sides of the no. 3 dam section model in the 2-D models, and were then constrained by the adjacent no. 2 and 4 sections for the 3-D models.
- The second one lies in the different definitions of the factor of safety. In the physical model tests, it is defined as the ratio between the maximum external load that is able to induce the sliding instability of the dam and the actual load designed to act on the

Table 6

Comparisons among the FEM and experimental results of the horizontal and vertical displacements at dam top, heel and toe of no. 3 powerhouse-dam section

Type	Displacements of dam top (mm)		Displacements of dam heel (mm)		Displacements of dam toe (mm)	
	Horizontal	Vertical	Horizontal	Vertical	Horizontal	Vertical
2-D FEM	10.94	−8.32	1.76	−0.55	1.63	−5.23
3-D FEM	3.85	−7.81	1.62	−4.35	1.52	−4.65
2-D physical Modeling	14.85	3.30	2.10	1.13	2.10	−0.37
3-D physical Modeling	11.74	2.1	1.85	0.95	1.20	−1.32

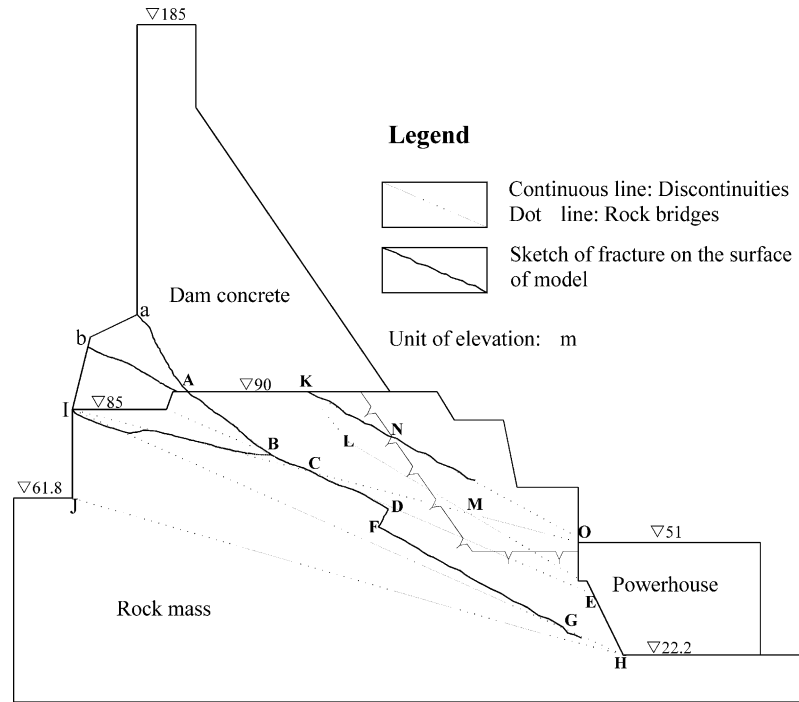


Fig. 18. Sketch of fracture traces on the model surface of the no. 3 powerhouse-dam section observed from the 2-D physical model test.

Table 7

Comparisons among the safety factors of no. 3 powerhouse-dam section derived from different analysis methods

	2-D FEM	3-D FEM	Limit equilibrium method	2-D physical modeling	3-D physical modeling
Safety factors	3.85	4.37	4.17	3.5	4.0

structure. However, in the numerical modeling, it is defined as the factor by which the shear strength parameters along the potential sliding planes may be reduced in order to bring the dam foundation into a state of limiting equilibrium.

- The third reason comes from the different simulations of the constitutive models and material properties. They were simulated by similarity of model materials in the physical model test, and by constitutive equations and associated material properties in the FEM modeling, which were not taken into account in the limit equilibrium method.

- Finally, the size effects probably also contributed to these differences of the factors of safety.

### 5. Overall assessments

The design and construction of the Three-Gorges Dam is unique. Its stability assessment has to be considered in terms of the particular circumstances of the site geological setting, properties and structures of rock mass, designed loads, and end uses for which it is intended. The stability assessment depends upon the

level of confidence that the designers/researchers have in the shear strength parameters and the locations of the potential failure surface. As presented in Part I of this combined paper, the geological settings and structures of the rock mass were adequately understood through numerous detailed geological investigations, and the properties of the rocks and discontinuities were identified by many of the field and laboratory tests. Following this, a geomechanical model was established by rational conceptualization. All these investigations provided a reliable basis for the stability analyses. Despite some differences in the results from the various approaches, both physical modeling and numerical modeling supported each other and produced complementary results, suggesting a stable dam foundation. The main assessment conclusions can therefore be made as follows.

- Under normal loading conditions, the concrete structure and foundation of the no. 3 dam section behave elastically and the deformations along the foundation surfaces are acceptable. Thus, the concerned dam foundation is stable under the designed normal loading conditions.
- The failure mechanisms are complicated. All the results suggested that in the foundation of the no. 3 powerhouse-dam section, *ABCDFGH* is the dominant sliding path, which, on the other hand, is resisted by both the upper concrete structure and the downstream powerhouse basement. Considering the limitation in all the numerical models that the foundation surfaces were pre-assumed as a part of the most critical potential sliding surface, thus leading to the *AK* section as the expanded part of *ABCDFGH* sliding path (Fig. 12(d)), the expanded paths *aA* and *bA* in the dam concrete revealed in the physical modeling should be more rational (Fig. 18). In addition, because the shear strengths along the interface between the powerhouse basement and the foundation are lower than that of the basement concrete, as revealed by both the numerical and physical modeling, the dominant sliding path *ABCDFGH* should be more easily extended downstream along the interface *HZ*. Therefore, the most critical sliding paths of the no. 3 section should be *aABCDFGHZ* and *bABCDFGHZ*.
- In this study, two definitions of the factor of safety were, respectively, used in physical and numerical modeling. The factor of safety in the physical modeling is defined as the ratio between the maximum external load inducing the start of sliding instability of the dam foundation and the upstream hydrostatic load applied to the dam, which reflects the failure mode due to external overload and the uncertainties of the upstream hydrostatic load. The experimental results show that the failure load is 3.5 times that of the designed load in the 2-D physical

model test and 4.0 in the 3-D physical model test. The factor of safety in the numerical modeling is defined as the factor by which the shear strength parameters may be reduced in order to bring the dam foundation into a state of limiting equilibrium, which indicates the another important failure mode due to the gradual degradation and the uncertainties of the shear strengths of discontinuities. The factor of safety computed by numerical modeling are 3.85 in 2-D FEM, 4.37 in 3-D FEM and 4.17 in Limit Equilibrium Method. In addition, the factors of safety derived from both the 2-D physical modeling and FEM are more conservative for the design than those from the corresponding 3-D analyses because the mutual constraint effects between the adjacent dam section foundations were not taken into account in the 2-D analyses.

As Hoek pointed out [15], there are no simple universal rules for design acceptability nor are there standard factors of safety, which can be used to guarantee that a rock structure will be safe and that it will perform adequately. A safe and economical solution should be compatible with all the constraints that apply to the dam and based upon engineering judgment guided by practical and theoretical studies such as stability or deformation analyses [15]. Based on numerous research results, the Chinese Design Criterion of Concrete Gravity Dam (in which the factor of safety against sliding of concrete gravity dam must be more than 3.0), the experience from design and construction of many similar projects in China, as well as the particular importance of the Three-Gorges Project, the Technical Committee of the Three-Gorges Project decided that the factor of safety against sliding of the Three-Gorges Dam must be higher than 3.0 [16–19]. Therefore, it can be concluded that the stability of the no. 3 powerhouse-dam section can meet the safety requirements because all the factors of safety derived from the multiple approaches are more than 3.0. In addition, since the foundation of the no. 3 powerhouse-dam section is the most critical in terms of stability against sliding failure (as demonstrated in Part I of this paper), a conclusion can be drawn that the global stability of the Three-Gorges Dam can also satisfy the safety requirements.

## 6. Treatment and reinforcement measures

Considering the importance of the Three-Gorges Project and the potential failure mechanisms revealed by the physical and numerical modeling, the following treatment and reinforcement measures for the foundation of the no. 3 powerhouse-dam section were suggested and implemented. Some adjustments of these

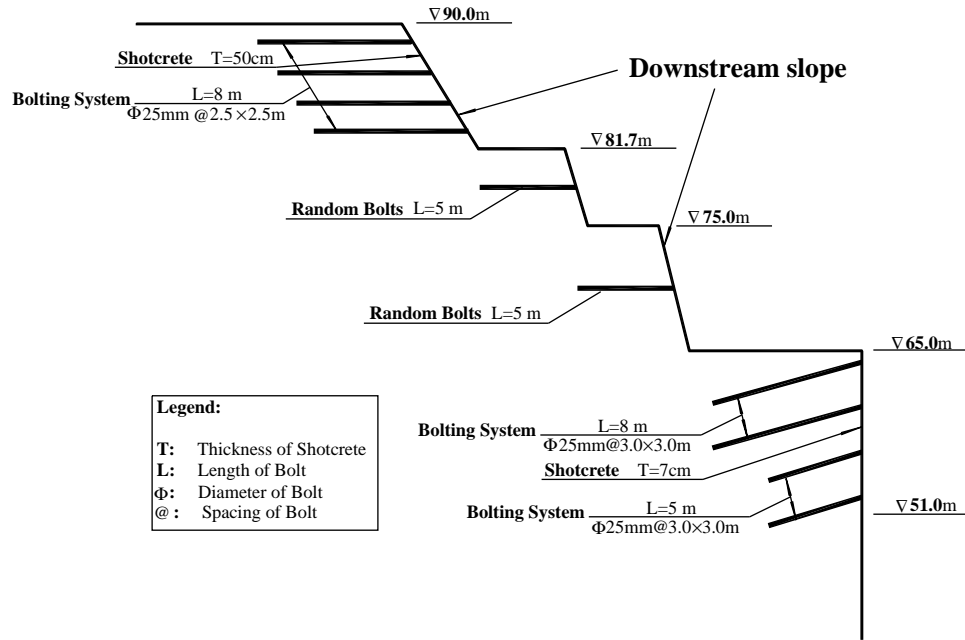


Fig. 19. Design scheme recommended for reinforcing the foundation of some critical dam sections of the Three-Gorges Dam.

measures may also be appropriate for other dam sections.

- (1) With the consideration that the mutual constraint effect between the adjacent foundations plays a helpful role in enhancing the global sliding-resistant capacities of these dam sections, it is suggested to set up key seating and grout between the transverse joints of the concrete of the no. 1–5 dam sections.
- (2) Tightly integrating the foundation with the powerhouse basement would make the basement more resistance to the sliding for most of the potential sliding paths. Thus, joint grouting for the interfaces between the excavated downstream slope and the upstream surface of the powerhouse basement will enhance the stability of this dam section.
- (3) To ensure the local stability of the downstream slope, bolting support should be adopted along its downstream free surface. Fig. 19 shows the recommended reinforcement scheme for the downstream slope with free surface.
- (4) Although the grouting curtain can effectively decrease the seepage uplift, the remaining seepage uplift, which was not fully taken into account in this study, would play a disadvantageous influence on the sliding-resistant capacity of the rock mass. Thus, a closed drain and pumping system should be constructed in the foundation.
- (5) It is necessary to implement grouting treatment for the shallow gentle dipping joints.

- (6) During the excavation of the foundation, it is important to minimize the damage in the rock mass caused by blasting.

## 7. Conclusions

This paper has benefited from a long-term research effort for the Three-Gorges Dam, which has involved the geomechanical conceptualization, 2-D and 3-D finite element analyses, limit equilibrium analyses, 2-D and 3-D physical model tests, the definition and computation of factors of safety, the comprehensive assessment of the stability, and, finally, the treatment and reinforcement schemes. Some conclusions of overall importance reached during this study are:

- (1) Comprehensive assessment in terms of the factor of safety, deformations and failure mechanisms of the no. 3 powerhouse-dam section demonstrate that the stability against sliding of this critical dam section can meet the safety requirements. Furthermore, since both the geological and geomechanical site characterization and numerical and physical modeling have revealed that the foundation of the no. 3 section is the most critical in terms of stability against sliding failure, it can be concluded that the global stability of the Three-Gorges Dam foundation also can be ensured.
- (2) The integration of multiple methods is shown to be a more effective approach for the stability analyses

of the Three-Gorges Dam foundation since no satisfactory individual method can be used alone to solve the problem. Mutual validation and complementary results derived from various methods make the stability assessment more reliable and rational.

- (3) Considering the particular importance of the Three-Gorges Project, some treatment and reinforcement measures for the foundations of some typical dam sections are necessary. Moreover, according to the failure mechanisms revealed, the treatments and reinforcements recommended in this paper were implemented and should effectively increase the foundation stability of these dam sections.
- (4) The systematic methodologies presented in this paper could be expanded into stability studies for other dam engineering with similar geomechanical conditions.

### Acknowledgements

The paper has been financially supported by the Three-Gorges Development Corporation, Changjiang Water Resources Commission, the Special Funds for Major State Basic Research Project under Grant no. 2002CB412708, the Pilot Project of Knowledge Innovation Program of Chinese Academy of Sciences under Grant no. KGCX2-SW-302-02, and National Natural Science Foundation of China under Grant no. 59939190. The authors wish to thank all colleagues in the Department of Structures & Materials, and Rock Foundation Department, Yangtze River Scientific Research Institute, for their valuable contributions to various parts of the works described in the paper, particularly Professors Gong Zhaoxiong Chen Jin and Sheng Qian. The authors also grateful to Prof. Lanru Jing, Royal Institute of Technology, Stockholm, Sweden, and Prof. J.A. Hudson for helping in preparing this paper.

### References

- [1] Liu J, Feng XT, Ding XL, Zhang J, Yue DM. Stability assessment of the Three-Gorges Dam foundation using physical and numerical modeling—Part I: physical modeling. *Int J Rock Mech Min Sci*, this issue.
- [2] Alonso E, Carol I, Delahaye C, Gens A, Prat P. Evaluation of factors of safety in discontinuous rock. *Int J Rock Mech Min Sci Geomech Abstr* 1996;33(5):513–37.
- [3] Jing L. Formulation of discontinuous deformation analysis (DDA)—an implicit discrete element model for block systems. *Eng Geol* 1998;49:371–81.
- [4] Duncan JM. State of the art: limit equilibrium and finite element analysis of slopes. *J Geotech Eng ASCE*, 1996;122(7):577–96.
- [5] Chen ZY, Wang XG, C, Haberfield C, Yin JH, Wang YJ. A three-dimensional slope stability analysis method using the upper bound theorem—Part I: theory and methods. *Int J Rock Mech Min Sci Geomech Abstr* 2001;38(3):369–78.
- [6] Shu YF. *Mechanics of materials*. Beijing: Chinese Higher Education Publishers, 1984. p. 289–305 [in Chinese].
- [7] Dhawan KR, Singh DN, Gupta ID. 2D and 3D finite element analysis of underground openings in an inhomogeneous rock mass. *Int J Rock Mech Min Sci* 2002;39(2):217–27.
- [8] Kovari K. *The elasto-plastic analysis in the design practice of underground openings*. London: Wiley; 1977.
- [9] Liu XZ. Experimental study on stiffness characteristics of rock mass structural face in TGP. *J Yangtze River Sci Res Inst, Wuhan, China* 1998;15(2):25–7 [in Chinese].
- [10] Dong XC. Experimental study on rock mechanical properties at Sandouping dam site in the Three-Gorges Project. *J Yangtze River Sci Res Inst, Wuhan, China*, 1992;(Suppl.)A06:13–21 [in Chinese].
- [11] Tian Y. Study on mechanical properties of rock mass of the Three-Gorges Project. *J Yangtze River Sci Res Inst, Wuhan, China*, 1992;(Suppl.)A06:72–6 [in Chinese].
- [12] Ding XL, Liu J, Liu XZ. Experimental study on creep behaviors of hard structural plane in TGP's permanent lock regions. *J Yangtze River Sci Res Inst, Wuhan, China* 2000;17(4):30–4 [in Chinese].
- [13] Zhou WY. *Senior rock mechanics*. Beijing: Chinese Water Conservancy and Hydro-electric Power Publishers, 1990. p. 53–6 [in Chinese].
- [14] Sun GR, Yin YQ, Qian ZG. Study on bearing capacity of concrete gravity dam. *J Hydraul Eng* 2001;4:15–20 [in Chinese].
- [15] Hoek E. *Practical rock engineering*, Course Notes on website: <http://www.rocsience/hoek/PracticalRockEngineering.asp>, 2000 [Chapter 2, p. 18–25].
- [16] Ministry of Water Conservancy and Hydro-electric Power. DL5108–1999 Chinese design criterion of concrete gravity dam. Beijing: Chinese Water Conservancy and Hydro-electric Power Publishers [in Chinese].
- [17] Yue DY, Jiang WQ, Liu JS. The comprehensive analysis of the stability against sliding of no. 1–no. 5 powerhouse dam sections of the Three-Gorges Dam. In: Research report, by Yangtze Water Resources Commission, Wuhan, China, 1997 [in Chinese].
- [18] Yue DY, Jiang WQ. The special design report of the foundation treatment of no. 1–no. 5 powerhouse dam sections of the Three-Gorges Dam. In: Research report, by Yangtze Water Resources Commission, Wuhan, China, 1996 [in Chinese].
- [19] Dong XC. Stability of the dam foundation, rock mass classification and optimization of the foundation line. In: Proceedings of the International Workshop on Rock Engineering Related to the Three-Gorges Project, Yichang, China, 1993.